[33]G. Tibell, A. Cowley, D. A. Goldberg, H. G. Pugh, W. Reichart, S. M. Smith, and N. S. Wall, Bull. Am. Phys. Soc. 17, 465 (1972); S. M. Smith *et al.*, Nucl. Phys. (to be published).

[34]L. N. Blumberg, E. E. Gross, A. van der Woude, A. Zucker, and R. H. Bassel, Phys. Rev. 147, 812 (1966).

[35]N. Austern and J. S. Blair, Ann. Phys. (N.Y.) 33, 15 (1965).

PHYSICAL REVIEW C VOLUME 7, NUMBER 5 MAY 1973

Nuclear Deformation of ^{28}Si from ^{16}O + ^{28}Si Elastic and Inelastic Scattering*

D. S. Gale† and J. S. Eck

Department of Physics, Kansas State University, Manhattan, Kansas 66506

(Received 21 July 1972)

Differential scattering cross sections for the elastic and first excited state inelastic scattering of ^{16}O and ^{18}O from ^{28}Si have been measured at ^{16}O laboratory bombarding energy of 33, 36, and 38 MeV and at an ^{18}O bombarding energy of 36 MeV. The experimental results have been analyzed in terms of coupled channels on the basis of a rotational model. For ^{16}O projectiles the deformation of ^{28}Si was found by this technique to be $\beta_2 = -0.30 \pm 0.08$ and $\beta_4 \geq +0.1$. The cross sections for the scattering of ^{18}O by ^{28}Si could not be described with the deformation parameters obtained from the ^{16}O + ^{28}Si scattering data. The present results are compared with recent experiments using different projectiles and with the results of recent theoretical calculations.

I. INTRODUCTION

It is generally recognized that the first half of the $2s$-$1d$ shell exhibits rotational behavior and is a region of ground-state deformation.[1-10] Recent nuclear structure calculations of the deformation parameters for nuclei in the $2s$-$1d$ shell have stimulated interest in the measurement of these parameters.[11-17] Such data are a critical test of these microscopic calculations. As early as 1957 it was suggested that ^{28}Si has a static oblate deformation.[18] Until recently, however, firm evidence was not available that this region of the s-d shell exhibits a static oblate deformation.[19]

In this paper we describe attempts to measure the deformation of ^{28}Si by coupled-channel analysis of the elastic and inelastic scattering cross sections of ^{16}O + ^{28}Si and ^{18}O + ^{28}Si at energies just above the Coulomb barrier. The main purpose of the present work is to investigate the deformation parameters β_2 and β_4 as a function of the incident particle energy and as a function of various incident particles. It has been previously shown that heavy-ion scattering just above the Coulomb barrier is dominated by surface interactions and therefore provides an excellent method for determining nuclear shapes.[20,21] The use of heavy projectiles such as ^{16}O in this energy range results in a wavelength of relative motion between target and projectile which is smaller than the nuclear surface distortions. The nuclear deformation parameters β_2 and β_4 obtained for ^{28}Si in the present work are compared to recent results obtained using other projectiles.[19,22-27]

II. EXPERIMENTAL PROCEDURE

In this work the elastic and first excited state inelastic differential scattering cross sections for the scattering of ^{16}O and ^{18}O by ^{28}Si were measured. The ^{16}O and ^{18}O beams used in these experiments were obtained from the Kansas State University Model EN tandem Van de Graaff accelerator. Beam energies from 27 to 40 MeV were used. The targets were self-supporting SiO_2 (99.58% enriched ^{28}Si). Target thickness varied from 70 to 120 μg/cm^2. The beam was triply collimated before entering a precision scattering chamber. The diameter of the beam spot on the target was less than 2 mm. Surface barrier detectors with sensitive depths of approximately 100 μm were used to detect the scattered particles. The detectors were mounted on movable arms and collimated so that in all cases they subtended less than 0.5° in the horizontal plane as viewed from the target.

Although kinematic coincidence between the scattered ^{16}O and the recoiling ^{28}Si was tried, this method was not found to be useful, since the multiple scattering of ^{28}Si in the target required that the ^{28}Si detector subtend a large solid angle to insure that all recoil particles were detected. The data reported in this work were obtained from singles spectra. Impurity peaks in the spectra resulting from various ^{16}O + ^{12}C reactions were eliminated by using self-supporting ^{28}Si targets, an oil free vacuum system, and detectors which were too thin to completely stop the resulting α particles. A typical singles scattering spectrum is shown in Fig. 1.

Elastic and first excited state inelastic differential scattering cross sections for the scattering of ^{16}O by ^{28}Si were measured at ^{16}O bombarding energies of 33, 36, and 38 MeV from 30 to 65° in the lab in 2.5° steps. In addition, elastic scattering differential cross sections were obtained for these energies at angles from 15 to 30° in the lab. The angular distribution for the scattering of ^{18}O by ^{28}Si was measured in a similar fashion at an ^{18}O bombarding energy of 36 MeV. Elastic scattering excitation functions for ^{16}O + ^{28}Si were measured at 40 and 60° in the lab. The ^{16}O bombarding energy ranged from 30 to 40 MeV in 0.5-MeV steps. The elastic and inelastic differential cross sections extracted at 40 and 60° at 40 MeV were in agreement with the data obtained by Siemssen.[26]

The areas under the elastic and inelastic peaks were normalized by measuring the elastic scattering from a small tungsten impurity which was present in all targets as a result of the evaporation of SiO_2 from a tungsten boat. The accuracy of this normalization technique was verified by comparison with beam current integration and by comparison with elastic scattering into a fixed monitor detector. Absolute cross sections were obtained by normalizing the elastic scattering yields to Rutherford cross sections at 15, 17.5, and 20°. The uncertainty in the absolute normalization was calculated to be less than 4%. The yields for the elastic and inelastic peaks were extracted using a computer program that fitted the data to two Gaussians with a quadratic background. The square of the uncertainty in the area of the inelastic peaks was taken to be $\sigma^2 = A + A_b$, where A equals the total area under the peak, including background, and A_b equals the area of the background. If the reduced χ^2 was greater than one, the square of the uncertainty was multiplied by the reduced χ^2. The uncertainty in the area of the elastic peaks was taken to be either 2% or as determined by the above criteria. The 2% minimum error was a result of the normalization procedure.

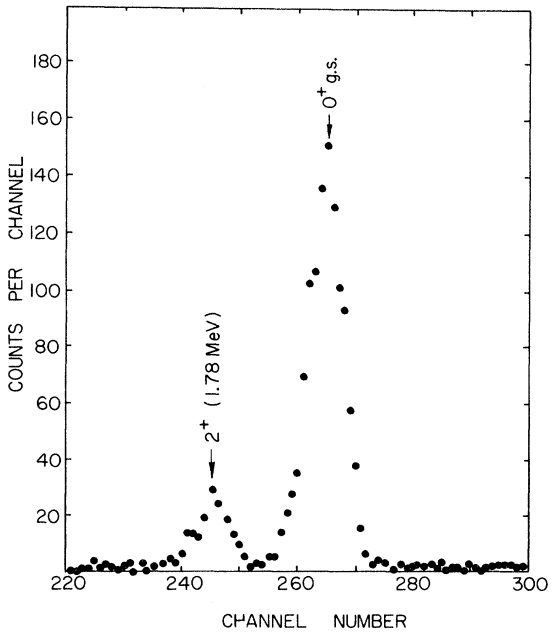

FIG. 1. Typical spectrum of the elastic, ^{28}Si(^{16}O,^{16}O)^{28}Si, and first excited state inelastic, ^{28}Si(^{16}O,^{16}O)^{28}Si*, scattering of 36-MeV ^{16}O from ^{28}Si at $\theta_{lab} = 57.5°$.

III. ANALYSIS AND RESULTS

A. Elastic Scattering

As a first step in the analysis, the elastic scattering cross sections were fitted using an optical-model potential of the form

$$V = V_C - \frac{V_0}{1+\exp[(r-R_0)/a_0]} - i\frac{W_0}{1+\exp[(r-R_0)/a_w]}, \quad (1)$$

where V_0 and W_0 are the real and imaginary poten-

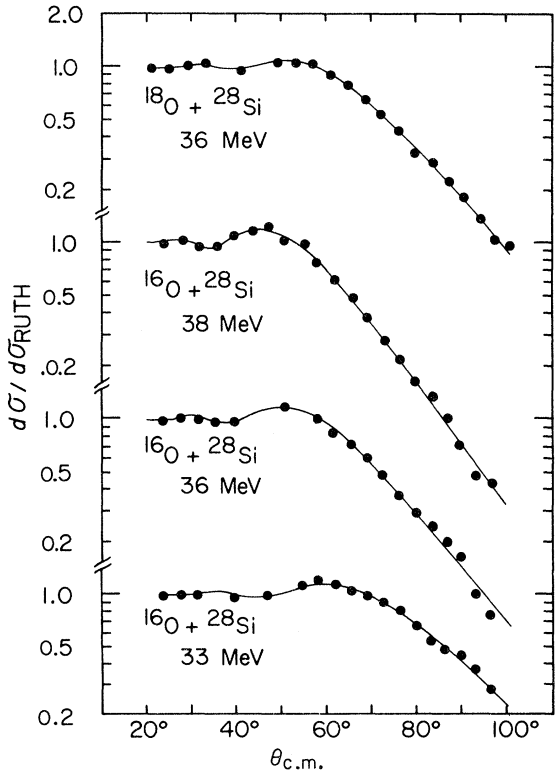

FIG. 2. Optical-model fits to the elastic scattering of ^{16}O and ^{18}O from ^{28}Si at various ^{16,18}O bombarding energies. The optical-model parameters are given in Table I.

tial strengths and a_0 and a_w are the real and imaginary diffuseness parameters. R_0 is the nuclear radius and is given by

$$R_0 = r_0(A_1^{1/3} + A_2^{1/3}) . \quad (2)$$

V_C is the Coulomb potential of a uniformly charged sphere and is given by

$$V_C(r) = \frac{Zze^2}{2R_0}\left[3 - (r/R_0)^2\right], \quad r < R_0$$

$$= \frac{Zze^2}{r}, \quad r \geq R_0 . \quad (3)$$

The parameters V_0, W_0, a_0, a_w, and r_0 were varied to obtain the best fits to the data. V_0 and W_0 parameter space was also searched for fixed a_0, a_w, and r_0 for $V_0 = 0$–300 MeV and $W_0 = 0$–100 MeV. Only one χ^2 minimum was found, indicating that there are no phase equivalent discrete ambiguities within this range of V_0 and W_0. The best fits for the angular distributions are shown in Fig. 2; the best fits to the excitation functions are shown in Fig. 3. The corresponding parameter values are given in Table I. Over the energy range investigated the optical model parameters were found to be independent of energy and consistent with the parameters used by Siemssen[26] to describe the elastic scattering of 40-MeV ^{16}O from ^{28}Si. These parameters were used as the starting point in the coupled-channels analysis.

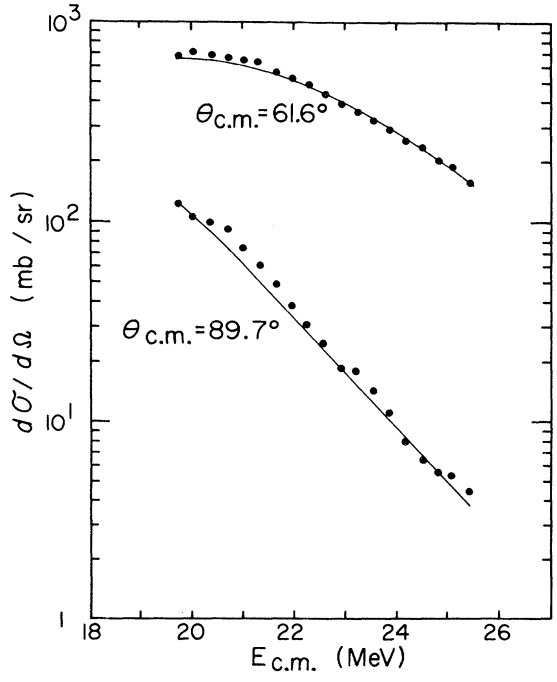

FIG. 3. Comparison of the $^{16}O + ^{28}Si$ elastic scattering excitation functions (points) with optical-model calculations using the same potential used in Fig. 2 (solid lines).

B. Inelastic Scattering

The next step in the analysis was to fit the inelastic cross sections simultaneously with the elastic cross sections by means of a coupled-channels code. This was done using the computer code JUPITER 1[28] on the CDC-3600 computer at Argonne National Laboratory. The ^{28}Si was assumed to be an axially symmetric deformed nucleus with a surface described as

$$R = R_0[1 + \beta_2 Y_{20}(\theta') + \beta_4 Y_{40}(\theta')] , \quad (4)$$

where θ' refers to the body fixed system. β_2 and β_4 represent the quadrupole and hexadecapole deformations of the ^{28}Si. In addition, the ground state (0^+), the first excited state (2^+ at 1.78 MeV), and the second excited state (4^+ at 4.61 MeV) were assumed to be members of the same rotational band. Coulomb excitation effects were explicitly included but found to be insignificant through 67 partial waves. The radial mesh size and matching radius were all chosen to insure high accuracy in the final results.

Initially, calculations were made on the $^{16}O + ^{28}Si$ cross sections for positive and negative values of β_2 with $\beta_4 = 0$. Even for small values of β_2 the inelastic cross sections were not proportional to $(\beta_2)^2$, indicating that a distorted-wave Born-approximation (DWBA) calculation is not suitable. These preliminary calculations indicated that β_2 had a value of approximately −0.3 or +0.2. The introduction of a small positive hexadecapole deformation (β_4) greatly improved the fits and indicated that for $\beta_2 > 0$ it was impossible to obtain calculated angular distributions which resemble the data. For values of $\beta_4 < 0$ the fits were worse in all cases. The influence of β_4 on the 2^+ cross sections was found to be around 20%. The optical-model parameters were then readjusted to compensate for the introduction of 0^+-2^+-4^+ coupling and the final values for β_2 and β_4 were determined by varying these parameters. By small variations in the optical-model parameters, it

TABLE I. Optical-model parameters for the elastic scattering of ^{16}O and ^{18}O from ^{28}Si.

Incident projectile	E_{lab} (MeV)	V_0 (MeV)	W_0 (MeV)	r_0 (fm)	a_0 (fm)	a_w (fm)
^{16}O	33.00	16.75	7.00	1.35	0.49	0.38
^{16}O	36.00	16.75	7.00	1.35	0.49	0.38
^{16}O	38.00	16.75	7.00	1.35	0.49	0.38
^{18}O	36.00	16.75	7.00	1.35	0.49	0.60

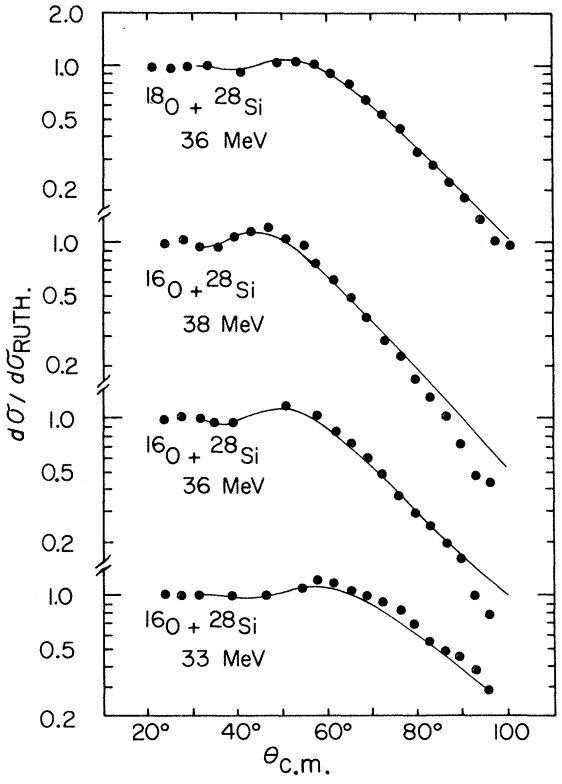

FIG. 4. Coupled-channel fits to the elastic scattering of ^{16}O and ^{18}O from ^{28}Si at various ^{16,18}O bombarding energies. The coupled-channel fits are for $\beta_2=-0.3$ and $\beta_4=+0.1$ with 0^+-2^+-4^+ coupling. Complete parameter specifications are given in Table II.

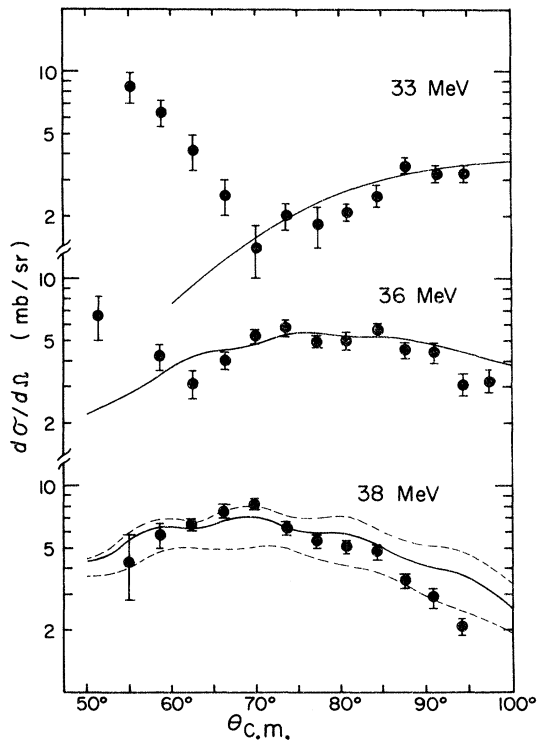

FIG. 5. Coupled-channel fits to the inelastic scattering of ^{16}O from ^{28}Si at various ^{16}O bombarding energies. The solid curves are for $\beta_2=-0.3$ and $\beta_4=+0.1$. The upper dashed curve is for $\beta_2=-0.38$ and $\beta_4=+0.1$; the lower dashed curve is for $\beta_2=-0.22$ and $\beta_4=+0.1$. 0^+-2^+-4^+ coupling was used in each case. Complete parameter specifications are given in Table II.

was possible to fit the inelastic scattering cross sections equally well with several values of β_2. It was not possible, however, to simultaneously fit both the elastic and inelastic scattering cross sections with these parameters. The fits to the elastic (0^+) scattering cross sections are shown in Fig. 4. The fits to the inelastic (2^+) scattering for ^{16}O + ^{28}Si* are shown in Fig. 5. It was found that no combination of parameters yielded the forward peaking evident in the 33- and 36-MeV data. In determining the best coupled-channels fits, no attempt was made to fit this forward peaking. The forward peaking will be considered further in the discussion. The values of the deformation parameters and optical-model parameters for the coupled-channels fits are given in Table II.

It proved to be impossible to fit the ^{18}O + ^{28}Si cross sections with the values of β_2 and β_4 obtained from the ^{16}O + ^{28}Si cross sections. The best fits to the ^{18}O + ^{28}Si cross sections that could be

TABLE II. Coupled-channel parameters for the elastic and inelastic scattering of ^{16}O and ^{18}O from ^{28}Si.

Incident projectile	E (MeV)	β_2	β_4	V_0 (MeV)	W_0 (MeV)	r_0 (fm)	a_0 (fm)	a_w (fm)
^{16}O	33.00	−0.30	+0.10	14.00	4.00	1.31	0.49	0.38
^{16}O	36.00	−0.30	+0.10	14.00	4.00	1.31	0.49	0.38
^{16}O	38.00	−0.22	+0.10	14.00	4.00	1.31	0.49	0.38
^{16}O	38.00	−0.30	+0.10	14.00	4.00	1.31	0.49	0.38
^{16}O	38.00	−0.38	+0.10	14.00	4.00	1.29	0.49	0.38
^{18}O	36.00	−0.30	+0.10	14.00	4.00	1.31	0.49	0.60
^{18}O	36.00	−0.38	+0.10	14.00	4.00	1.31	0.49	0.38

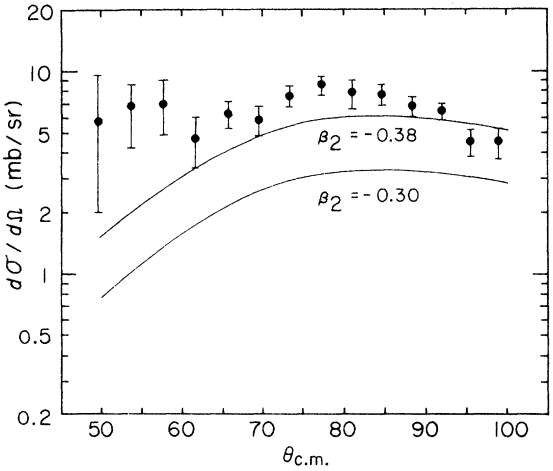

FIG. 6. Coupled-channel fits to the inelastic scattering of ^{18}O from ^{28}Si for $\beta_2 = -0.38$ and $\beta_4 = +0.1$ and for $\beta_2 = -0.30$ and $\beta_4 = +0.1$. 0^+-2^+-4^+ coupling was used in both cases. Complete parameter specifications are given in Table II.

obtained with the deformation parameters determined from the $^{16}O + ^{28}Si$ data are shown in Fig. 6. The corresponding optical-model parameters are given in Table II.

The results of this work as well as the results of other recent experiments and theoretical calculations are given in Table III. The intrinsic quadrupole moment of ^{28}Si can be calculated from β_2 and β_4. If we assume a homogeneous charge distribution for a nucleus with a surface defined by Eq. (4), the intrinsic quadrupole moment may be expressed as[29]

$$Q_{20} = \frac{3}{\sqrt{5\pi}} ZR_0^2(\beta_2 + 0.360\beta_2^2 + 0.328\beta_4^2 + 0.967\beta_2\beta_4). \quad (5)$$

This value has been computed for our results using $R_0 = 1.35A^{1/3}$ and is included in Table III. Since there is some question as to whether β, Q, or the deformation length βR is the correct parameter to compare, the quantity $\beta_2 R$ has also been included in Table III.

IV. DISCUSSION

The present work indicates that the scattering of ^{16}O from ^{28}Si at energies just above the Coulomb barrier is sensitive to the surface features of ^{28}Si and may be partially described in terms of a coupled-channel calculation based on a rotational model of the ^{28}Si nucleus. In general the deformation parameter β_2 obtained for ^{28}Si using electrons, protons, α particles, and ^{16}O as projectiles are in agreement, but are inconsistent with the β_2 obtained using deuterons or ^{18}O as a bombarding projectile. One possible explanation for this inconsistency is the fact that electrons, protons, α particles, and ^{16}O projectiles are not readily polarized by the nuclear encounter and

TABLE III. Experimental and theoretical results for the deformation of ^{28}Si.

Method	β_2	β_4	$\beta_2 R$	Q_{20} (b)	Reference
(^{16}O, $^{16}O'$) CC [a]	-0.30 ± 0.08	$\geq +0.1$	-1.19	-0.54 ± 0.13	Present work
(α, α') CC	-0.26 ± 0.08	$\lvert\beta_4\rvert \leq 0.1$	-1.11		27
(α, α') CC	-0.32 ± 0.01	$+0.08 \pm 0.01$	-1.34	-0.47 ± 0.02	19
(d, d') CC	-0.52		-1.41		23
(p, p') CC	-0.34	$+0.25$	-1.28		22
$B(E2,\ 0^+ \text{-} 2^+)$				0.56 ± 0.04	24
$Q(2^+)$ [b]				-0.59 ± 0.18	24
(e, e')	-0.39	$+0.10$		-0.64 ± 0.03	25
(^{14}N, $^{14}N'$) DWBA	0.174		1.24		26
(^{15}N, $^{15}N'$) DWBA	0.158		1.17		26
(^{16}O, $^{16}O'$) DWBA	0.148		1.12		26
HF [c]				-0.49	10
SM [d]				-0.56	11
HF	-0.29				12
HF				-0.84	13
HF				-0.92	14
HF				-0.50 to -0.61	15
PES [e]				-0.54	16
HF				-0.72	17

[a] CC, coupled-channel analysis.
[b] $Q(2^+)$ by reorientation effect.
[c] HF, Hartree-Fock calculation.
[d] SM, shell-model calculation.
[e] PES, potential energy surface calculation.

effectively act as structureless point particles, while the deuterons and ^{18}O projectiles are readily polarized and thus their structure must be considered in any meaningful coupled-channel analysis of the scattering cross section. This interpretation is consistent with recent evidence[30] for the ground-state deformation of ^{18}O.

Although it is not expected that a DWBA analysis of scattering cross sections from highly deformed nuclei such as ^{28}Si would have much validity, it can be seen from Table III that the DWBA analysis of the scattering of ^{16}O, ^{15}N, and ^{14}N projectiles from ^{28}Si shows the deformation of parameter β_2 tending towards larger values as the incident projectile is further removed from a closed shell.

The angular distributions for the scattering of ^{16}O from ^{28}Si at 33, 36, and 38 MeV are all equally well described by the same values of β_2, β_4, and optical-model parameters. This indicates that β_2 and β_4 have no large energy dependence over this energy range.

The notable characteristic of the 33- and 36-MeV inelastic scattering angular distributions is the peaking at forward angles, followed by a distinct minima, followed in turn by a "hump." This minima occurs roughly at the point where $\sigma_{el}/\sigma_{Ruth}$ falls below unity. Videvaek *et al.*[31] have recently observed the same signature for ^{58}Ni(^{16}O,^{16}O)^{58}Ni*. They interpret their results in terms of interference between Coulomb and nuclear excitation, with Coulomb excitation dominating in the region of forward peaking. An explicit calculation of Coulomb excitation in the region below the Coulomb barrier, however, indicated that Coulomb excitation, although appreciable, may be a factor of 2 smaller than the differential cross sections observed in the present work. Thus, although Coulomb excitation may not entirely explain the forward peaking in the present work, it does indicate that a coupled-channels calculation must consider appreciably more than 67 partial waves to describe data in the region just below the Coulomb barrier. The values of β obtained in the present work were obtained by fitting data above the Coulomb barrier where the nuclear potential is assumed to dominate. A second possible explanation for the forward peaking observed in the 33- and 35-MeV data is that ^{28}Si and ^{16}O may undergo additional deformation during the interaction. Presumably this would be more pronounced at forward angles.

Comparison between the present experimental results and theoretical calculations is difficult, since Eq. (5) is only correct to the second order in β_2 and β_4. In general there is reasonable agreement between the present experimental results and theoretical calculations.

The inelastic scattering of ^{16}O at energies just above the Coulomb barrier has been shown to reveal the surface features of ^{28}Si. The relative simplicity of these measurements suggests the applicability of this technique to the measurement of nuclear shapes. The resolution of higher multipole orders would probably require analysis of the 4^+ inelastic cross sections, the inclusion of the finite size, and the possibility of the internal excitation of the ^{16}O projectile.

The authors are deeply indebted to Professor W. J. Thompson of the University of North Carolina at Chapel Hill for invaluable assistance with the coupled-channel code.

---

*Work performed under contract AT(11-1)-2130 with the U.S. Atomic Energy Commission.

†Present address: Department of Physics, East Texas State University, Commerce, Texas 75428.

[1]H. E. Gove, in *Proceedings of the International Conference on Nuclear Structure, Kingston, 1960*, edited by D. A. Bromley and E. W. Vogt (Univ. Toronto Press, Toronto, Canada, 1960), p. 436.

[2]H. Grawe and K. P. Lieb, Nucl. Phys. **A127**, 13 (1969).

[3]J. A. Anderson and R. C. Ritter, Nucl. Phys. **A128**, 305 (1969).

[4]F. C. P. Huang and D. K. McDaniels, Phys. Rev. C **2**, 1342 (1970).

[5]M. M. Aleonard, D. Castera, P. Hubert, F. Leccia, P. Mennrath, and J. P. Thibaud, Nucl. Phys. **A146**, 90 (1970).

[6]K. Nakai, J. L. Quebert, F. S. Stephens, and R. M. Diamond, Phys. Rev. Lett. **24**, 903 (1970).

[7]K. Nakai, F. S. Stephens, and R. M. Diamond, Nucl. Phys. **A150**, 114 (1970).

[8]D. Pelte, O. Häusser, T. K. Alexander, and H. C. Evans, Can. J. Phys. **47**, 1929 (1969).

[9]D. Pelte, O. Häusser, T. K. Alexander, B. W. Hooton, and H. C. Evans, Phys. Lett. **29B**, 660 (1969).

[10]G. Ripka, in *Advances in Nuclear Physics*, edited by M. Baranger and E. Vogt (Plenum, New York, 1968), Vol. I, pp. 183–259.

[11]B. H. Wildenthal, J. B. McGrory, and P. W. M. Glaudemans, Phys. Rev. Lett. **26**, 96 (1971).

[12]A. P. Stamp, Nucl. Phys. **A105**, 627 (1967).

[13]B. Castel and J. C. Parikh, Phys. Lett. **29B**, 341 (1969).

[14]B. Castel and J. P. Svenne, Nucl. Phys. **A127**, 141 (1969).

[15]B. Castel and J. C. Parikh, Phys. Rev. C **1**, 990 (1970).

[16]I. Ragnarsson and S. G. Nilsson, Nucl. Phys. **A158**, 155 (1970).

[17]J. Zofka and G. Ripka, Nucl. Phys. **A168**, 65 (1971).

[18]D. A. Bromley, H. E. Gove, A. E. Litherlaud, Can. J. Phys. **35**, 1057 (1957).

[19]H. Rebel, G. W. Schweimer, G. Schatz, J. Specht, R. Löhken, G. Hauser, D. Habs, and H. Klewe-Nebenius, Nucl. Phys. **A182**, 145 (1972).

[20]J. S. Eck and W. J. Thompson, in *Proceedings of the*

International Conference on Nuclear Reactions Induced by Heavy Ions, Heidelberg, Germany, 1969, edited by R. Bock and R. Herring (North-Holland, Amsterdam, 1970), pp. 85–88.
[21]M. Samuel and U. Smilansky, Phys. Lett. **28B,** 318 (1968).
[22]R. de Swiniarski, C. Glashausser, D. L. Hendrie, J. Sherman, A. D. Bacher, and E. A. McClatchie, Phys. Rev. Lett. **23,** 317 (1969).
[23]M. C. Mermaz, C. A. Whitten, and D. A. Bromley, Phys. Rev. **187,** 1466 (1969).
[24]O. Hässer, T. K. Alexander, D. Pelte, B. W. Hooton, and H. C. Evans, Phys. Rev. Lett. **23,** 320 (1969).
[25]Y. Horikawa, Y. Torizuka, A, Nakada, S. Mitsunobu, Y. Kojima, and M. Kimura, Phys. Lett. **36B,** 9 (1971).
[26]R. H. Siemssen, in *Proceedings of the Symposium Heavy-Ion Scattering, Argonne National Laboratory, 1971* (Argonne National Laboratory, Argonne, Ill., 1971).
[27]A. W. Obst and K. W. Kemper, Phys. Rev. C **6,** 1705 (1972).
[28]T. Tamura, Oak Ridge National Laboratory Report No. ORNL-4152, 1967 (unpublished).
[29]R. Winkler, in *Proceedings International Conference on Nuclear Reactions Induced by Heavy Ions, Heidelberg, 1969* (See Ref. 20), p. 464.
[30]F. Resmini, R. M. Lombard, M. Pignanelli, J. L. Escudie, and A. Tarrats, Phys. Lett.**37B,** 275 (1971).
[31]F. Videbaek, I. Chernov, P. R. Christensen, and E. E. Gross, Phys. Rev. Lett. **28,** 1072 (1972).

PHYSICAL REVIEW C VOLUME 7, NUMBER 5 MAY 1973

Electromagnetic Transition Rates in ^{38}Cl and ^{40}K

G. H. Wedberg*
Argonne National Laboratory, Argonne, Illinois 60439, and Indiana University, Bloomington, Indiana 47401

Ralph E. Segel
Argonne National Laboratory, Argonne, Illinois 60439,† and Northwestern University, Evanston, Illinois 60201‡

(Received 8 November 1972)

The attenuated-Doppler-shift method was used to measure the mean lives of low-lying states in ^{38}Cl and ^{40}K. States were populated by the (d,p) reaction and the recoil direction was defined by coincidence with the outgoing proton. While the positions of the levels in these two nuclei give encouragement to the belief that many of the states are well described as members of simple particle-hole or particle-particle multiplets, it is immediately apparent that the magnetic dipole transition rates do not fit the simple picture even if effective moments are used. A recent theoretical study has shown that some admixtures that can be expected will significantly alter the $M1$ rates, but the present results are not in good agreement with the theoretical predictions. Other available lifetime data on these nuclei support the present contention that there are severe discrepancies between the observed rates and those predicted by the best available shell-model calculations.

INTRODUCTION

The nuclei ^{38}Cl and ^{40}K provide an interesting testing ground for the shell model. In the simple shell-model picture in which ^{40}Ca is a doubly-closed-shell nucleus, ^{38}Cl is described by the configuration $(\pi d_{3/2})(\nu f_{7/2})$, and ^{40}K by the configuration $(\pi d_{3/2})^{-1}(\nu f_{7/2})$, each configuration producing a quartet of states. At a low excitation in each nucleus, the shell model predicts another quartet of negative-parity states of the $(\pi d_{3/2})^{\pm1}(\nu p_{3/2})$ configuration. Since this model is successful in predicting many of the gross features of the low-lying ^{38}Cl and ^{40}K levels, it is worthwhile to start applying the more stringent test of comparing electromagnetic transition rates with the theoretical predictions.

Our measurements of the $M1$ rates of transitions among members of the ground-state quartet in each nucleus were not in agreement with the simple picture.[1] The present report on the measurement of the lifetimes of a number of higher states completes our study of these two nuclides. In the interim, transition rates in ^{38}Cl and ^{40}K have been reported by several other groups: Wechsung *et al.*[2] reported on transitions in ^{40}K that proceed from levels up to 2.626-MeV excitation energy, James *et al.*[3] measured the lifetimes of ^{40}K levels up to 3.153-MeV excitation energy, and Engelbertink and Olness[4] studied the levels of ^{38}Cl up to an excitation energy of 2.743 MeV.

The ^{39}K$(d,p)^{40}$K reaction has been studied by Enge, Irwin, and Weaner[5] and more recently by Fink.[6] A study of the ^{37}Cl$(d;p)^{38}$Cl reaction has been reported by Rapaport and Buechner.[7] Early theoretical work[8,9] showed that the energy of the lowest four levels in one of these nuclei could be accurately predicted from the position of the low-